

1 Atropos: specific, sensitive, and speedy 2 trimming of sequencing reads

3 John P Didion¹, Marcel Martin², and Francis S Collins¹

4 ¹National Human Genome Research Institute, National Institutes of Health, Bethesda,
5 MD

6 ²Science for Life Laboratory, Department of Biochemistry and Biophysics, Stockholm
7 University, Sweden

8 Corresponding author:

9 John P Didion, PhD¹

10 Email address: john.didion@nih.gov

11 ABSTRACT

12 **Summary.** A key step in the transformation of raw sequencing reads into biological insights is the
13 trimming of adapter sequences and low-quality bases. Read trimming has been shown to increase
14 the quality and reliability while decreasing the computational requirements of downstream analyses.
15 Many read trimming software tools are available; however, no tool simultaneously provides the accuracy,
16 computational efficiency, and feature set required to handle the types and volumes of data generated in
17 modern sequencing-based experiments. Here we introduce Atropos and show that it trims reads with high
18 sensitivity and specificity while maintaining leading-edge speed. Compared to other state-of-the-art read
19 trimming tools, Atropos achieves a four-fold increase in trimming accuracy and a decrease in execution
20 time of up to 40% (using 16 parallel execution threads). Furthermore, Atropos maintains high accuracy
21 even when trimming data with elevated rates of sequencing errors. The accuracy, high performance, and
22 broad feature set offered by Atropos makes it an appropriate choice for the pre-processing of Illumina,
23 ABI SOLiD, and other current-generation short-read sequencing datasets. **Availability.** Atropos is open
24 source and free software written in Python (3.3+) and available at [https://github.com/jdidion/](https://github.com/jdidion/atropos)
25 [atropos](https://github.com/jdidion/atropos).

26 1 INTRODUCTION

27 All current-generation sequencing technologies, including Illumina, ABI SOLiD, and Ion Torrent, require
28 a library construction step that involves the introduction of short adapter sequences at the ends of the
29 template DNA fragments. Depending on the sequencing platform and the fragment size distribution of
30 the sequencing library, an often substantial fraction of reads will consist of both template and adapter
31 sequences (Figure 1A). Additionally, the error rates of these sequencing technologies vary from ~0.1% on
32 Illumina to 5% or more on long-read sequencing platforms. Error rates tend to be enriched at the ends
33 of reads (where adapters are located), thus exacerbating the effects of adapter contamination. Adapter
34 contamination and sequencing errors can lead to increased rates of misaligned and unaligned reads, which
35 results in errors in downstream analysis including spurious variant calls (Del Fabbro et al., 2013; Sturm
36 et al., 2016). Certain sequencing protocols may introduce other artifacts in sequencing reads. For example,
37 some methylation sequencing (Methyl-Seq) protocols result in artificially methylated bases at the 3' ends
38 of reads that can lead to inflated estimates of methylation levels (Bock, 2012).

39 Read trimming is an important step in the analysis pipeline to mitigate the effects of adapter contami-
40 nation, sequencing errors, and other artifacts. The development of tools for read trimming is an active
41 area of bioinformatics research, thus there are currently many options. In terms of adapter trimming, these
42 tools fall into two general categories: 1) those that rely solely on matching the adapter sequence (*adapter-*
43 *match trimming*) using semi-global alignment (which is the only option available for single-end reads;
44 Figure 1B); and 2) those that leverage the overlap between paired-end reads to identify adapter starting
45 positions (*insert-match trimming*; Figure 1C) (Sturm et al., 2016). Cutadapt (Martin, 2011) is a mature
46 and feature-rich example of a tool that provides adapter-match trimming, while SeqPurge (Sturm et al.,

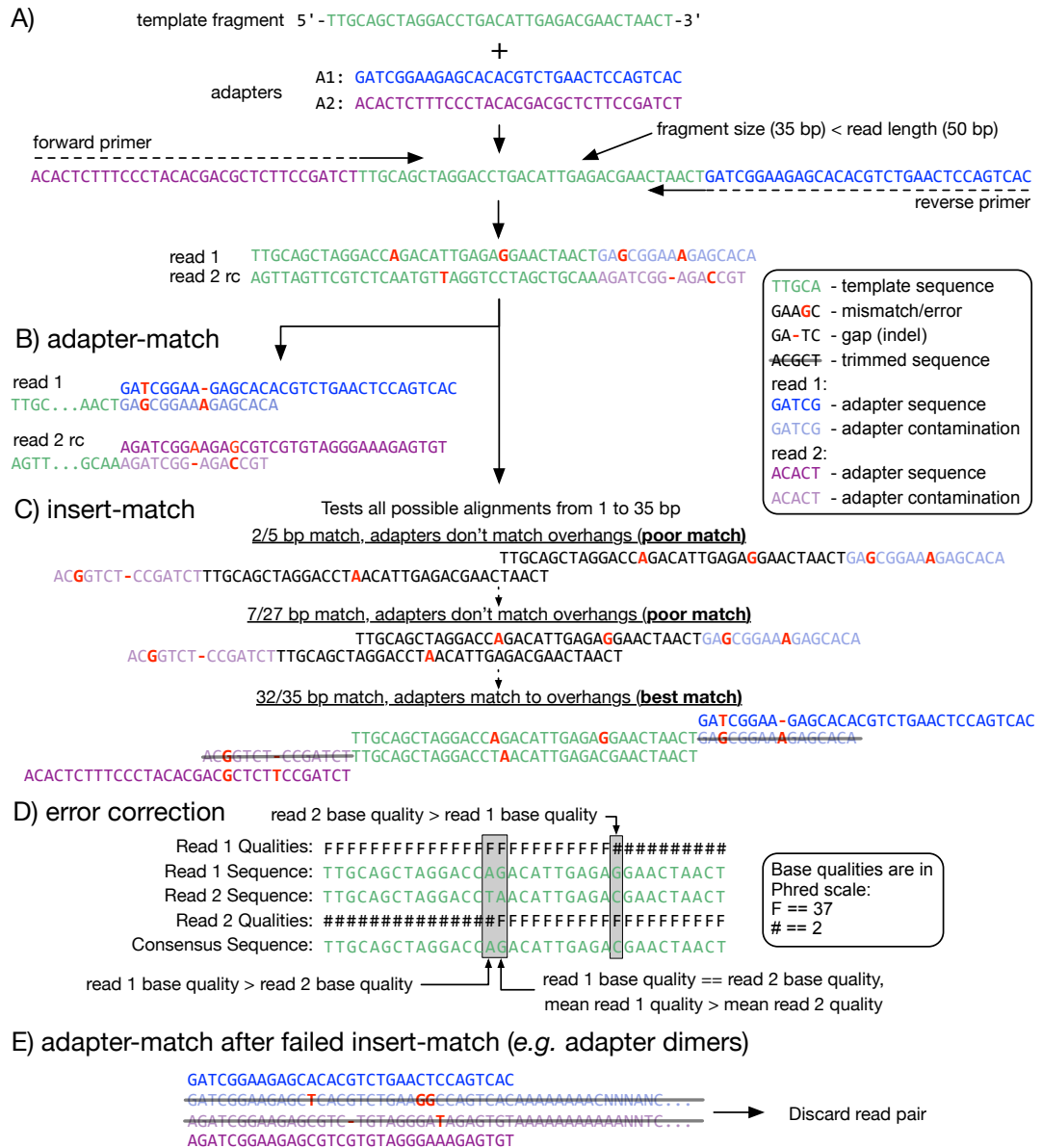


Figure 1. Adapter detection and trimming. A) When a fragment (or insert; green) is shorter than the read length, the read sequence will contain partial to full-length adapter sequences (blue and purple). B,C) Methods for detecting adapter contamination using semi-global alignment. Adapter-match (B) identifies the best alignment between each adapter and the end of its corresponding read. Insert-match (C) first identifies the best alignment between read 1 and the reverse-complement (rc) of read 2; if a valid alignment is found, then adapters are matched to the remaining overhangs. D) If a match is found, the overlapping inserts can be used for mutual error correction. The consensus base is the one with the highest quality, or, if the bases have equal quality, the one from the read with highest mean quality. E) If insert-match fails (for example, with an adapter dimer) adapter-match is performed. Reads that are too short after trimming are discarded.

47 2016) is a recent example of a highly accurate insert-match trimmer designed specifically for paired-end
 48 data. Additionally, hybrid tools are available that optimize their choice of read trimming method based
 49 on the type of data. Skewer (Jiang et al., 2014) and AdapterRemoval (Version 2) (Schubert et al., 2016)
 50 are fast and accurate hybrid trimmers that works with both single-end and paired-end data. However,

51 choosing a read-trimming tool currently requires a trade-off between feature set, efficiency, and accuracy.
52 Furthermore, even state-of-the-art tools still have a relatively high rate of over-trimming (removing usable
53 template bases from reads) and/or under-trimming (leaving low-quality and adapter-derived bases in the
54 read sequence) (Sturm et al., 2016).

55 We sought to develop a read trimming tool that would combine the best aspects of currently available
56 software to provide high speed and accuracy while also offering a rich feature set. To accomplish this aim,
57 we used Cutadapt as a starting point, as it provides the broadest feature set of currently available tools and
58 is published under the MIT license, which allows modification and improvement of the code. We focused
59 on making three specific improvements to Cutadapt: 1) improve the accuracy of paired-end read trimming
60 by implementing an insert-match algorithm; 2) improve the performance by adding multiprocessing
61 support (as **Cutadapt is currently only able to use a single processor**); and 3) add important additional
62 features such as automated trimming of Methyl-Seq reads, automated detection of adapter sequences in
63 reads where the experimental protocols are not known to the analyst, estimation of sequencing error, and
64 generation of quality control (QC) metrics. Because these modifications required substantial changes to
65 the Cutadapt code base, and because there are software tools that depend on the current implementation
66 of Cutadapt, we chose to “fork” the Cutadapt code base and develop our software, Atropos, as a separate
67 tool. Here, we show that we have accomplished our three aims. In addition to extending the already rich
68 set of features provided by the original Cutadapt tool, Atropos demonstrates paired-end read trimming
69 accuracy that is superior to other state-of-the-art tools, and it is among the fastest read trimming tools
70 when a moderate number of parallel execution threads are used (4). Furthermore, Atropos achieves a
71 performance increase that is roughly linear with the number of threads used, making it the fastest tool
72 when 8 or more threads are available.

73 2 MATERIALS AND METHODS

74 2.1 Implementation

75 Atropos is developed in **Python (3.3+)** and is available to install from GitHub or via one of several package
76 managers (see Data Availability).

77 2.1.1 Semi-global Alignment

78 Traditionally, the overlap between two sequences is detected by computing an optimal semi-global
79 alignment (Gusfield, 1997, Section 11.6.4), which is the same as global alignment except that neither
80 initial nor trailing gaps are penalized. This allows the sequences to shift relative to each other. An optimal
81 semi-global alignment maximizes the sum of alignment column scores, thus tending to favor longer over
82 short overlaps. Since score-based optimization is often not intuitively understood, the adapter alignment
83 algorithm uses edit operations instead, which has the advantage that it gives the user the ability to specify
84 a “maximum error rate” **as an intuitive parameter**. For a given alignment between read and adapter, the
85 error rate is computed as the number of edits (mismatches, insertions, deletions) divided by the length of
86 the matching part of the adapter. Minimizing the edit distance while at the same time not penalizing end
87 gaps would lead to optimal but meaningless zero-length overlaps; thus, a hybrid approach is chosen. The
88 adapter alignment algorithm computes edit distances for all allowed shifts of the adapter relative to the
89 read. Among those having an error rate not higher than the specified threshold, the shift (and therefore
90 alignment) with the highest number of matches is chosen.

91 **We summarize the algorithm here; see (Martin, 2013, Section 2.2) for details. Let a and r be the**
92 **nucleotide sequences of the adapter and sequencing read, respectively, and let $m = |a|$, $n = |r|$. Adapter**
93 **alignment computes edit distances $D(i, j)$ between the i -length prefix of a and the j -length prefix of r for**
94 **all $i = 0, \dots, m$ and $j = 0, \dots, n$ with the standard dynamic-programming (DP) recurrence**

$$D(i, j) = \min\{D(i-1, j-1) + [a_i \neq r_j], D(i-1, j), D(i, j-1)\} \quad (1)$$

95 The base cases are $D(i, 0) = 0$ or $D(i, 0) = i$ and $D(0, j) = 0$ or $D(0, j) = j$, depending on the adapter
96 type, allowing to skip a prefix of a and/or r at no cost. The algorithm additionally keeps track of $M(i, j)$,
97 which is the number of matches between the prefixes of a and r , and of the “origin” $O(i, j)$, which is
98 the number of skipped characters in r in the optimal alignment (if negative, characters in a are skipped
99 instead). All three DP matrices D, M, O are filled in at the same time, after which the cells of the bottom
100 row ($i = m$) are inspected. They represent possible end positions of the adapter sequence within the

101 read. For each position j , the error rate is computed from $D(m, j)$ and $O(m, j)$, and positions with a too
102 high error rate are discarded. If positions remain, the one with the highest number of matches $M(m, j)$
103 is returned as the position J of the adapter sequence. Together with the start of the adapter sequence at
104 $O(m, J)$, the adapter sequence can then be removed from the read.

105 Observing that no backtrace within the DP matrix is required, the actual implementation keeps only
106 a single column of the matrices in memory for better cache locality. Significant runtime improvements
107 are achieved by employing the optimization described by Ukkonen (Ukkonen, 1985) of stopping the
108 computation of a column as soon as the costs are too high and provably cannot decrease for the remainder
109 of the column. When the user supplies an anchored adapter and disables insertions and deletions (indels)
110 at the same time, the algorithm also switches to a much simpler variant that computes only the Hamming
111 distance between the adapter and a prefix or suffix of the read.

112 **2.1.2 Insert Match Algorithm**

113 For each read pair, the insert-match algorithm uses the same semi-global alignment algorithm described
114 above (with indels disabled) to find all possible alignments between the first read and the reverse
115 complement of the second read that satisfy user-specified specificity thresholds (Figure 1C). Specificity
116 is determined by the combination of up to three user-configurable thresholds: 1) minimum number of
117 overlapping bases, 2) maximum number of mismatch bases, and 3) random mismatch probability (Sturm
118 et al., 2016). The probability of a random match at k bases out of the n bases being compared is computed
119 using the binomial distribution:

$$P = \sum_{i=k}^n \frac{n!}{i!(n-i)!} p^i (1-p)^{n-i} \quad (2)$$

120 The candidate alignments are tested in order of decreasing length until one is found in which the
121 overhanging sequences on either end match the user-specified adapter sequences. Comparison between
122 the adapter and overhang sequences is done using a constrained adapter-match approach. Briefly, starting
123 at the end of the insert overlap, a pairwise comparison is made between the adapter and the read at each
124 possible offset. The offset that best satisfies the user-configurable specificity thresholds (the same three
125 described above) is taken to be the location of the adapter sequence, and all bases from that position to the
126 3' end of the read are removed. If an adapter is only found in one of the two reads, then the same offset is
127 used to trim both reads, under the assumption that the location of the adapter sequence must be symmetric
128 across the read pair.

129 Optionally, the overlapping inserts can be used for mutual error correction (Figure 1D). Where the
130 aligned inserts have mismatches, the base with the highest quality score is chosen as the consensus. When
131 the bases have equal quality, there is an option to leave the bases unchanged, convert them both to N, or
132 to choose the base from the read with the highest mean quality as the consensus. There are additional
133 options to 1) completely overwrite one read in the pair if its quality is very poor, and/or 2) merge the
134 overlapping read pair into a single read, which avoids double-counting overlapping read pairs in read
135 depth-based analyses.

136 If no insert match is found, or if an adapter is not found in an overhang, then an unconstrained
137 adapter-match approach is attempted separately in each read (Figure 1E).

138 **2.1.3 Parallel processing**

139 The performance improvements in Atropos relative to Cutadapt and other read trimming tools are based in
140 two observations: 1) each read (or read pair) is trimmed separately, and thus trimming can be parallelized
141 across multiple processor cores, and 2) a significant fraction of the execution time is spent decompressing
142 input files and re-compressing results. Compression of sequencing data is increasingly becoming necessary
143 due to the large volumes of data generated in sequencing experiments.

144 To address the first bottleneck, we implemented a parallel processing pipeline based on the Python
145 multiprocessing module. Briefly, a single thread is dedicated to a “reader” process that loads reads (or
146 read pairs) from input file(s), with support for a variety of data formats and automatic decompression of
147 compressed data. Reads are loaded in batches, and each batch is added to an in-memory queue. A user-
148 specified number of “worker” threads (which is constrained by the number of processing cores available
149 on the user’s system) extract batches from the queue and perform trimming and filtering operations
150 on the reads in the same manner as Cutadapt. Atropos addresses the second bottleneck by offering a

151 choice of three modes for writing the results to disk. The first two modes involve adding the results
 152 to a second in-memory queue, from which a dedicated “writer” process extracts batches and performs
 153 the serialized write operation. These two modes differ in how the trimmed reads are compressed – in
 154 worker-compression mode, each worker is responsible for compressing the results using the Python gzip
 155 module prior to placing the results on the queue, whereas in writer-compression mode, the writer process
 156 performs compression using the much faster system-level gzip program. The choice between these two
 157 modes is selected automatically based on the number of worker threads used, with worker-compression
 158 mode becoming faster than writer-compression mode when at least 8 threads are available. The third
 159 output mode, called “parallel writing,” does not use a dedicated writer process (and thus an additional
 160 worker process can be used in its place). Instead, each worker process writes its results to a separate file.
 161 This can dramatically reduce the execution time of the program (~50% reduction in our experiments; see
 162 Results) and is generally compatible with downstream analysis since many mapping and assembly tools
 163 accept multiple input files (and for those that don’t, gzipped files can be safely concatenated without
 164 needing to be decompressed and recompressed). An additional speed-up is gained by recognizing that the
 165 reader process often finishes loading data well before the worker processes finish processing it; thus, an
 166 additional worker thread is started as soon as the reader process completes.

167 **2.1.4 Adapter detection**

168 Often, details of sequencing library construction are not fully communicated from the individual or facility
 169 that generated the library to the individual(s) performing data analysis. For example, the majority of
 170 datasets in the NCBI Sequence Read Archive (SRA) lack adapter sequence annotations. Manual determi-
 171 nation of sequencing adapters and other potential library contaminants can be a tedious and error-prone
 172 task. Thus, we implemented in Atropos a command that automatically identifies adapters/contaminants
 173 from a sample of read sequences. First, a profile is built of k -mers (where k is a fixed number of consecu-
 174 tive nucleotides, defaulting to $k = 12$) within N read sequences (where N defaults to 10,000). When at
 175 least 8 consecutive A bases are detected, those bases along with all subsequent bases (in the 3’ direction)
 176 are first trimmed, as that pattern is a strong indicator that the sequencer scanned past the end of the
 177 template (i.e. the length of the fragment + adapter is less than the read length; Figure 1E). Additionally,
 178 low-complexity reads are excluded, where complexity $X(S)$ is defined as follows. Let $C(i, S)$ be the
 179 number of elements of a nucleotide sequence $S = s_1, \dots, s_n$, that are nucleotide $i \in A, C, G, T$.

$$X(S) = - \sum \frac{C(i, S) \cdot \log(C(i, S))}{\log(2)} \quad (3)$$

180 Sequences with $X(S) < 1.0$ are defined as low-complexity. All remaining k -mers are counted, and
 181 each k -mer is linked to all of the sequences from which it originated. This process continues iteratively for
 182 increasing values of k , with only those read sequences linked to high-abundance k -mers in the previous
 183 iteration being used to build the k -mer profile in the next iteration. k -mer K is considered high-abundance
 184 when:

$$|K| > \frac{N \cdot (l - k + 1) \cdot O}{4^k} \quad (4)$$

185 where l is the read length and $O = 100$ by default. Finally, high-abundance k -mers of all lengths are
 186 merged to eliminate shorter sequences that are fully contained in longer sequences.

187 Atropos reports to the user an ordered list of up to 20 of the most likely contaminants. Because
 188 adapter sequences have been designed not to match any known sequence in nature, a sequence (or pair of
 189 sequences) that occurs at high frequency and matches a known adapter sequence is likely to be the true
 190 sequence(s) used as adapters in the dataset. Thus, our algorithm optionally matches the high-abundance
 191 k -mers to a list of known adapters/contaminants. We provide a list of commonly used adapter sequences,
 192 or the user can choose to supply their own. **When a contaminant list is not provided, or when the adapter
 193 does not match a known sequence, we advise the user to take caution when using the results of this
 194 detection process, as a highly abundant sequence might simply be derived from a frequently repeated
 195 element in the genome.**

196 **2.1.5 Error Rate Estimation**

197 Quality and adapter trimming is sensitive to the choice of several parameters. For example, relative to
198 datasets with typical rates of sequencing error, datasets with higher error-rates require higher thresholds
199 for mismatches and/or random-match probability during insert- and adapter-matching to perform with the
200 same level of sensitivity. Thus, we implemented in Atropos a command that provides an estimate of the
201 error rate in each input file. The error command gives the choice between two algorithms: 1) averaging all
202 base qualities across a sample of reads, which is fast but likely overestimates the true rate of sequencing
203 error (Dohm et al., 2008; DePristo et al., 2011); and 2) the shadow regression method proposed by Wang
204 *et al.* (Wang et al., 2012), which more accurately estimates error rates at the cost of reduced speed and
205 greater memory usage.

206 **2.1.6 Quality Control Metrics**

207 Examination of QC metrics is another important aspect of sequence analysis pipeline. For example,
208 the widely used FastQC (Andrews, 2010) tool generates statistics such as per-sequence and per-base
209 quality scores and GC content, sequence length distribution, sequence duplication levels, and frequency
210 of potential contaminants. QC is commonly performed both before and after read trimming to identify
211 any systematic data quality issues, to observe the improvements in data quality due to trimming, and to
212 ensure that trimming does not introduce any unintended side-effects. Since both read trimming and QC
213 involve iterating over all reads in the dataset, we reasoned that implementing both operations in the same
214 tool would reduce the overall processing time, and also eliminate the need to install two separate tools.
215 Thus, we implemented an option in Atropos to collect QC metrics before and/or after trimming.

216 Additionally, we implemented an Atropos module for MultiQC (Ewels et al., 2016), a program that
217 generates nicely formatted reports from metrics output by a variety of bioinformatics tools for one to many
218 samples. Given summary files generated by Atropos (one per sample, in JSON format), the MultiQC
219 module will generate interactive versions of the same static plots offered by FastQC, as well as a summary
220 table of the most important metrics.

221 **2.1.7 Shared Cutadapt and Atropos Improvements**

222 In addition to improvements in the semi-global alignment algorithm above, Atropos also benefits from the
223 following improvements that were made to Cutadapt subsequent to the publication of Martin *et al.* (2011),
224 but prior to the Atropos fork, and are therefore features in both programs.

- 225 • Adapters can now be *anchored*, which limits the read positions at which they will be matched. An
226 anchored 5' adapter thus matches only if it is a prefix of the read, and a 3' adapter only if it is a
227 suffix of the read. This is useful, for example, when one or both sequencing adapters are known to
228 be ligated directly to a PCR primer.
- 229 • *Linked adapters* combine a 5' with a 3' adapter. Trimming multiple adapters from each read was
230 also supported previously, but linked adapters make it possible to require that one of them is a 5'
231 adapter and one a 3' one.
- 232 • *IUPAC ambiguity codes* are fully supported. Thus, adapter sequences containing characters such
233 as N (matching any nucleotide), H (A, C, or T), Y (C or T) work as expected. They are useful
234 when adapters contain barcodes or random nucleotides. The nucleotides and ambiguity codes are
235 internally represented as patterns of four bits, in which each set bit corresponds to an allowed
236 nucleotide. Comparisons are thus simple “binary and” operations, resulting in no runtime overhead.
- 237 • *Paired-end data* can be trimmed with sequences specified for the forward and reverse reads
238 independently. Read pairs are guaranteed to remain in sync. Even *interleaved* data (paired-end
239 reads in a single file) is accepted.
- 240 • Quality trimming can now work in a *NextSeq-specific* mode in which spurious runs of high-quality
241 G nucleotides at the 3' end of a read are *correctly* trimmed. NextSeq instruments use “dark” or
242 “black” cycles for G nucleotides, making them unable to distinguish between regular G and reaching
243 the end of the fragment.
- 244 • Other additions include support for *trimming a fixed number of bases* from a read, support for files
245 compressed using the bzip2 and lzma algorithms, and improved filtering options.

246 **2.2 Benchmarks**

247 **2.2.1 Simulated Data**

Data Set	Error Rate*	Read Length	Total Read Pairs	Reads w/ Adapters**	Adapter Bases**
Simulated 1	0.20%	125	781,923	325,982	12,447,262
Simulated 2	0.60%	125	780,899	325,105	12,416,861
Simulated 3	1.20%	125	782,237	325,860	12,464,235
GM12878 WGBS	2.79%	125	1,000,000	57,130	3,082,003
K562 mRNA-seq	4.31%	75	6,100,265	14,384	749,451

Table 1. Description of data sets. For the real data sets, * actual error rates are unknown – we estimate error rates from base qualities over a sample of 10,000 read pairs; and ** total adapter content is unknown – we provide the number of reads containing exact matches for the first 35 adapter bases, and the number of adapter bases present.

248 We evaluated both the speed and the accuracy of Atropos relative to other state-of-the-art read
 249 trimming tools using both simulated and real-world data (Table 1). As trimming of single-end reads
 250 is unchanged from the original Cutadapt method and is also decreasing in relevance as most current
 251 experiments use paired-end data, we focused our benchmarking on trimming of paired-end reads. Sturm
 252 *et al.* demonstrate that Skewer (Jiang *et al.*, 2014) and SeqPurge (Sturm *et al.*, 2016) stand out as having
 253 superior performance in paired-end read trimming, and Schubert *et al.* also demonstrate exceptional
 254 performance of AdapterRemoval (Schubert *et al.*, 2016); thus, we chose to benchmark Atropos against
 255 these tools. We also compared the new insert-match algorithm against the adapter-match algorithm that is
 256 used by Cutadapt, and which can be enabled in Atropos using the ‘-aligner’ command line option.

257 To simulate paired-end read data, we use the ART simulator (Huang *et al.*, 2012) that was modified
 258 by Jiang *et al.* to add adapter sequences to the ends of simulated fragments. ART simulates reads based
 259 on empirically derived quality profiles specific to each sequencing platform. A quality profile consists
 260 of distributions of quality scores for each nucleotide at each read position, expressed as read counts
 261 aggregated from multiple sequencing experiments, where quality scores are in Phred scale ($-10\log_{10}(e)$,
 262 where e is the probability that the base call is erroneous). We developed an R script to artificially inflate
 263 the error rates in an ART profile to a user-defined level. For each row in the profile with quality score bins
 264 $e_1..e_n$ and corresponding read counts $r_1..r_n$, the overall error rate can be computed as:

$$E = \frac{\sum_{i=1}^n e_i r_i}{\sum_{i=1}^n r_i} \quad (5)$$

265 We use the R function *optim* with the variable metric (“BFGS”) algorithm to optimize a function
 266 that adds an equal number of counts C to each Phred-score bin in the distribution and then compares the
 267 overall error rate to the user-desired error rate E' :

$$f(C, E') = \frac{\sum_{i=1}^n e_i (r_i + C)}{\sum_{i=1}^n (r_i + C)} - E' \quad (6)$$

268 We simulated ~800k 125 bp paired-end reads using the Illumina 2500 profile at error rates that were
 269 low/typical (~0.2%, the unmodified profile), intermediate (~0.6%), and high (~1.2%). We evaluated the
 270 accuracy of the tools on the simulated data by comparing each trimmed read pair to the known template
 271 sequence. We counted the frequency of following outcomes: the fragment does not contain adapters but is
 272 trimmed anyway (“wrongly trimmed”), or the fragment does contain adapters but either too few bases or
 273 too many bases were removed (“under-trimmed” or “over-trimmed”). We also counted the total number
 274 of under- and over-trimmed bases.

275 **2.2.2 Real Data**

276 We also benchmarked the tools on two real-world datasets. First, we sampled ~1M read pairs from a
 277 whole-genome bisulfite sequencing (WGBS) library generated from the GM12878 cell line. Second, we
 278 used 6.1M paired-end mRNA-seq reads generated from the K562 cell line. Both of these datasets were

279 generated by the ENCODE project (ENCODE Project Consortium, 2012). Since the genomic origins of
280 the templates are not known *a priori*, we instead compared the read trimming tools based on improvement
281 in the results of mapping the trimmed versus untrimmed reads. We used STAR (Dobin et al., 2013) to
282 map the mRNA-seq reads to GRCh38, and we used bwa-meth (Pedersen et al., 2014) to map the WGBS
283 reads to the bisulfite-converted GRCh38. We also compared the results of only adapter trimming to the
284 results of adapter trimming plus additional quality trimming using a minimum quality threshold of 20
285 (Phred-scale).

286 One characteristic of the mRNA-Seq dataset is that average read 2 quality is substantially lower than
287 read 1 (estimation by the 'atropos error' subcommand: 6.7% vs 2.0%). In practice, when encountering
288 a read pair in which one end is of much lower quality than the other, the Skewer algorithm essentially
289 overwrites the former with the later, leading to more precise alignment. Atropos provides a specific option
290 for this case ('-w'), which we make use of in our benchmark in order to fairly compare Atropos with
291 Skewer. However, this gives these tools a perhaps unfair advantage over AdapterRemoval and SeqPurge
292 which do not have such an option.

293 **2.2.3 Computing Environments**

294 Although sequence analysis is sometimes performed using a desktop computer, analysis of the volumes of
295 data currently being generated increasingly requires the use of high-performance computing facilities
296 ("clusters"). The hardware architecture of a cluster is often different from that of a desktop computer. Most
297 importantly, storage in a cluster is typically centralized and accessed by the compute nodes via high-speed
298 networking. Such an architecture inevitably adds latency to file reading and writing operations ("I/O").
299 Cluster nodes also typically have more processing cores and memory available than desktop computers.
300 This means that the performance of software with intensive I/O usage (such as read trimming) is likely to
301 be quite different on a desktop versus a cluster. To examine the impact of these architectural differences,
302 we ran the benchmarks for simulated data on both a desktop computer (a Mac Pro) having a 3.7 GHz
303 quad-core Intel Xeon E5 processor and 32 GB RAM, and on a cluster node having 64 2.4 GHz Intel
304 Xeon E5 cores and 256 GB memory, and with all data being read from and written to network-accessible
305 storage over a 1 Gbit ethernet connection.

306 **2.2.4 Reproducibility and Reusability**

307 With increasing importance being placed on both the reproducibility of results in scientific publications
308 and the reusability of software and pipelines, we endeavored to provide a benchmark workflow that can
309 be easily executed and extended by anyone with access to modern computing resources.

310 First, we "containerized" all of the software tools used in this paper – including trimming tools,
311 read mapping tools, and supplementary tools used to evaluate results and generate tables and figures
312 (Supplementary Table 1). We also created minimal containers for all of the data used in this paper –
313 including benchmark datasets, reference genomes, annotation databases, and indexes used by the mapping
314 tools. Specifically, we created Docker (Boettiger, 2015) image specifications ("Dockerfiles"), generated
315 the images, and uploaded them to a public repository on the Docker Hub (see Data Availability).

316 Second, we implemented our benchmark workflow using the Nextflow (Di Tommaso et al., 2017)
317 framework. Importantly, Nextflow enables workflows to be run either locally or in most cluster environ-
318 ments, and supports running containerized software via either a Docker or Singularity (Kurtzer, 2016)
319 client (depending on the operating system).

320 Instructions for running our workflow, along with all of the source scripts, are available in our GitHub
321 repository (see Data Availability).

322 **3 RESULTS**

323 **3.1 Simulated Data**

324 **3.1.1 Performance**

325 On a desktop computer with 4 processing cores, we found that AdapterRemoval had the fastest overall
326 execution time, followed closely by SeqPurge, Atropos (in parallel write mode), and Skewer (Figure 2A
327 and Supplementary Table 2).

328 As expected, execution times on a cluster node using 4 threads were approximately 20% greater than
329 those observed on a desktop computer (Figure 2B and Supplementary Table 3). We expect that much of
330 this disparity is due to the increased latency involved in network-based I/O on the cluster, although some

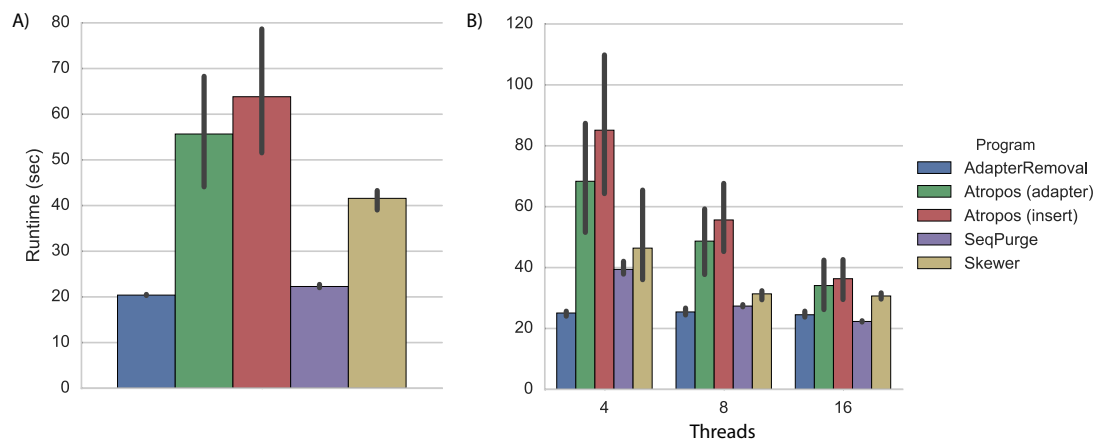


Figure 2. Trimming execution time for simulated data. Execution time on simulated datasets for programs running on A) a desktop computer with 4 parallel processes (threads), and B) a cluster node with 4, 8, and 16 threads. Each program was executed multiple times, and Atropos was run with combinations of alignment algorithm (insert-match or adapter-match) and output mode (**worker-compression, writer-compression or parallel-write**). The mean execution times for each program are shown with 95% confidence intervals.

331 may also be explained by CPU differences (3.7 GHz Intel on the desktop versus 2.4 GHz on the cluster
 332 node).

Program	Reads				Bases		
	Wrongly Trimmed	Over-trimmed	Under-trimmed	Total Error	Over-trimmed	Under-trimmed	Total Error
Error rate 0.2%							
AdapterRemoval	664 (0.09%)	29 (0.00%)	65 (0.01%)	0.10%	6,043	2,511	0.005%
Atropos (adapter)	51 (0.01%)	1 (0.00%)	28,991 (3.77%)	3.78%	490	102,133	0.057%
Atropos (insert)	60 (0.01%)	24 (0.00%)	31 (0.00%)	0.01%	186	94	0.000%
SeqPurge	94 (0.01%)	24 (0.00%)	31 (0.00%)	0.02%	1,574	94	0.001%
Skewer	18 (0.00%)	13 (0.00%)	146 (0.02%)	0.02%	39	8,309	0.005%
Error rate 0.6%							
AdapterRemoval	666 (0.09%)	19 (0.00%)	69 (0.01%)	0.10%	5,547	2,032	0.004%
Atropos (adapter)	72 (0.01%)	6 (0.00%)	28,843 (3.76%)	3.77%	733	101,839	0.057%
Atropos (insert)	52 (0.01%)	15 (0.00%)	42 (0.01%)	0.01%	151	146	0.000%
SeqPurge	78 (0.01%)	16 (0.00%)	41 (0.01%)	0.02%	822	145	0.001%
Skewer	8 (0.00%)	8 (0.00%)	180 (0.02%)	0.03%	16	11,732	0.007%
Error rate 1.2%							
AdapterRemoval	680 (0.09%)	16 (0.00%)	65 (0.01%)	0.10%	5,795	2,667	0.005%
Atropos (adapter)	76 (0.01%)	5 (0.00%)	30,152 (3.92%)	3.94%	721	117,027	0.065%
Atropos (insert)	49 (0.01%)	13 (0.00%)	35 (0.00%)	0.01%	111	85	0.000%
SeqPurge	71 (0.01%)	13 (0.00%)	35 (0.00%)	0.02%	1,524	85	0.001%
Skewer	11 (0.00%)	8 (0.00%)	182 (0.02%)	0.03%	19	14,261	0.008%

Table 2. Trimming accuracy on simulated data with three different base-call error rates. **Wrongly trimmed:** reads that do not contain adapters but were trimmed anyway; **Over-trimmed:** reads that contain adapters but from which too many bases were removed; **Under-trimmed:** reads that contain adapters but from which too few bases were removed. Both read-level and base-level error rates are shown. Fractions of total reads/bases are in parentheses. The best tool(s) in each category is highlighted.

333 When increasing the number of parallel execution threads from 4 to 8 and 16, Atropos achieves
334 a roughly linear decrease in execution time. Interestingly, the execution times of AdapterRemoval,
335 SeqPurge, and Skewer do not substantially decrease when increasing the number of the threads from 8 to
336 16. With 8 and 16 threads, Atropos using the adapter-match algorithm in parallel-write mode is the fastest
337 of the tools, and with 16 threads Atropos using the insert-match algorithm in parallel-write mode is also
338 faster than the other three tools (Supplementary Table 3).

339 Atropos uses substantially more memory than the other tools (Supplementary Figure 1 and Supple-
340 mentary Table 4). We expect this is partially due to overhead of automatic memory management in Python
341 compared to C++ (in which AdapterRemoval, SeqPurge, Skewer are implemented), but in larger part
342 results from Atropos' use of in-memory queues to communicate between parallel processes. For all four
343 programs, memory usage increases slightly with increasing number of threads. We note that Atropos
344 provides parameters to limit memory usage (although typically at the expense of reduced speed).

345 For most datasets and thread counts, Atropos and Skewer typically achieve the highest mean CPU
346 utilization, indicating that they are less I/O-bound than AdapterRemoval or SeqPurge (Supplementary
347 Figure 2).

348 **3.1.2 Accuracy**

349 We found that the four trimming algorithms had different biases toward under- and over-trimming
350 (Table 2). Across the three sequencing error rates, Skewer had the lowest frequency of wrongly trimming
351 reads while AdapterRemoval had the highest. The Atropos adapter-match algorithm exhibited almost no
352 over-trimming of reads, but also had a very high frequency of under-trimming. The Atropos insert-match
353 algorithm and SeqPurge had similarly low frequencies of under-trimming reads. Overall, the Atropos
354 insert-match algorithm demonstrated the lowest error rates at the read level (0.01%).

355 In terms of numbers of over- and under-trimmed bases, the Atropos insert-match algorithm and
356 SeqPurge clearly had the best performance (Table 2) at all sequencing error rates. The two algorithms
357 had similarly low numbers of under-trimmed bases, but the Atropos insert-match algorithm had a lower
358 number of over-trimmed bases, giving it the lowest overall error rate (0.0002%). On the other hand,
359 Skewer and the Atropos adapter-match algorithm left substantial numbers of under-trimmed bases while
360 AdapterRemoval was again biased towards over-trimming.

361 Additionally, we found that all tools discarded very similar numbers of reads (~1.8%) that were below
362 the minimum length threshold of 25 bp after trimming. These were reads with short insert sizes, which
363 have a high rate of spurious mapping, and thus it is common practice to discard them.

364 **3.2 Real Data**

365 We first tested Atropos' adapter detection module on the real datasets. Using the first 10,000 reads in each
366 pair of FASTQ files, Atropos correctly detected the exact sequences of the adapters used in constructing
367 each library. For 3 of the 4 adapters, the sequences were found in a list of known contaminants (WGBS
368 read 1: "TruSeq Adapter, Index 7"; WGBS read 2 and mRNA-seq read 2: "TruSeq Universal Adapter");
369 the mRNA-seq read 1 adapter appears to have a custom-designed sequence.

370 **3.2.1 Performance**

371 We performed adapter trimming on the real datasets in the same cluster environment. Again, we found that
372 AdapterRemoval had the fastest execution time (Figure 3 and Supplementary Tables 5-6). When trimming
373 the WGBS data with 16 threads, Atropos (using the insert-match algorithm in parallel-write mode) was
374 nearly as fast as AdapterRemoval (Figure 3A and Supplementary Tables 5), while on the mRNA-Seq
375 data Skewer, SeqPurge, and Atropos were all 30-50% slower than AdapterRemoval (Figure 3B and
376 Supplementary Tables 6).

377 We also performed read mapping on the cluster with 16 cores. Mapping times were very similar for
378 all algorithms on both the WGBS and mRNA-Seq datasets, and were much faster than for the untrimmed
379 reads (Supplementary Figure 3).

380 **3.2.2 Effectiveness**

381 We assessed read trimming effectiveness in practical terms. For the WGBS data, we computed the number
382 of trimmed reads mapped at a given quality (MAPQ) cutoff, relative to the number of untrimmed reads
383 mapped at that cutoff. We found that trimming by Atropos resulted in the greatest increase in number of
384 mapped reads at all quality cutoffs (Figure 4A). Trimming with SeqPurge, Skewer, and AdapterRemoval

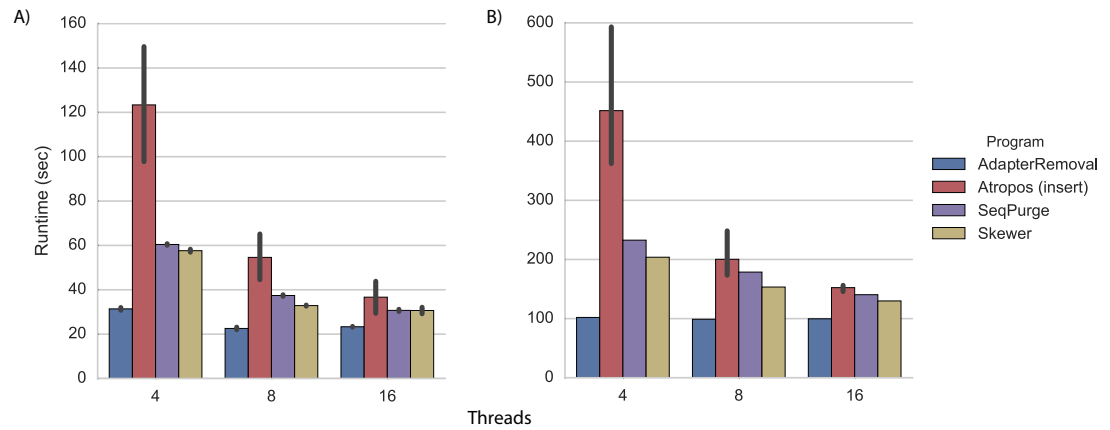


Figure 3. Trimming execution time for real data. Execution time on real datasets for programs running on a cluster node with 4, 8, and 16 threads. Each program was executed multiple times, and Atropos was run with the insert-match algorithm and parallel-write output mode. The mean execution times for each program are shown with 95% confidence intervals.

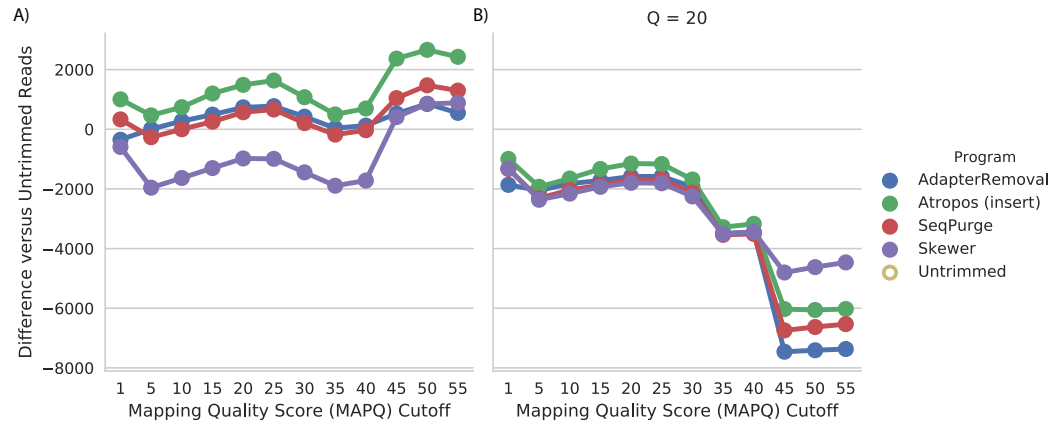


Figure 4. Atropos trimming best improves mapping of real WGBS sequencing reads. Reads were adapter-trimmed with all four programs A) without additional quality trimming ($Q=0$) and B) with quality trimming at a threshold of $Q=20$. We mapped both untrimmed and trimmed reads to the genome. For each MAPQ cutoff $M \in \{0, 5, \dots, 60\}$ on the x-axis, the number of trimmed reads with $\text{MAPQ} \geq M$ less the number of untrimmed reads with $\text{MAPQ} \geq M$ is shown on the y-axis for each program.

385 resulted in similar, but smaller, gains in mapping quality. At the highest MAPQ thresholds (45, 50, 55),
 386 Atropos substantially outperforms the other three tools.

387 We also found that additional quality trimming in addition to adapter trimming has a substantial
 388 negative effect on read mapping, at least for bisulfite reads mapped using bwa-meth (Figure 4B). Quality
 389 trimming by Skewer had the least negative effect on mapping quality of the four programs, and quality
 390 trimming by AdapterRemoval had the greatest negative effect on mapping quality.

391 For the mRNA-seq data, we additionally compared each alignment to **GENCODE (v26)** gene annotations
 392 (Harrow et al., 2012) to determine the number of reads mapped to expressed regions of the genome.
 393 We found that trimming with Atropos resulted a greater number of mapped reads aligned to expressed
 394 regions compared to the other tools at all MAPQ thresholds (Figure 5).

395 4 CONCLUSIONS

396 Our results demonstrate that adapter trimming tools are approaching optimal accuracy, at least for the
 397 (currently) most common type of data – paired-end short reads with 3' adapters. On synthetic data with

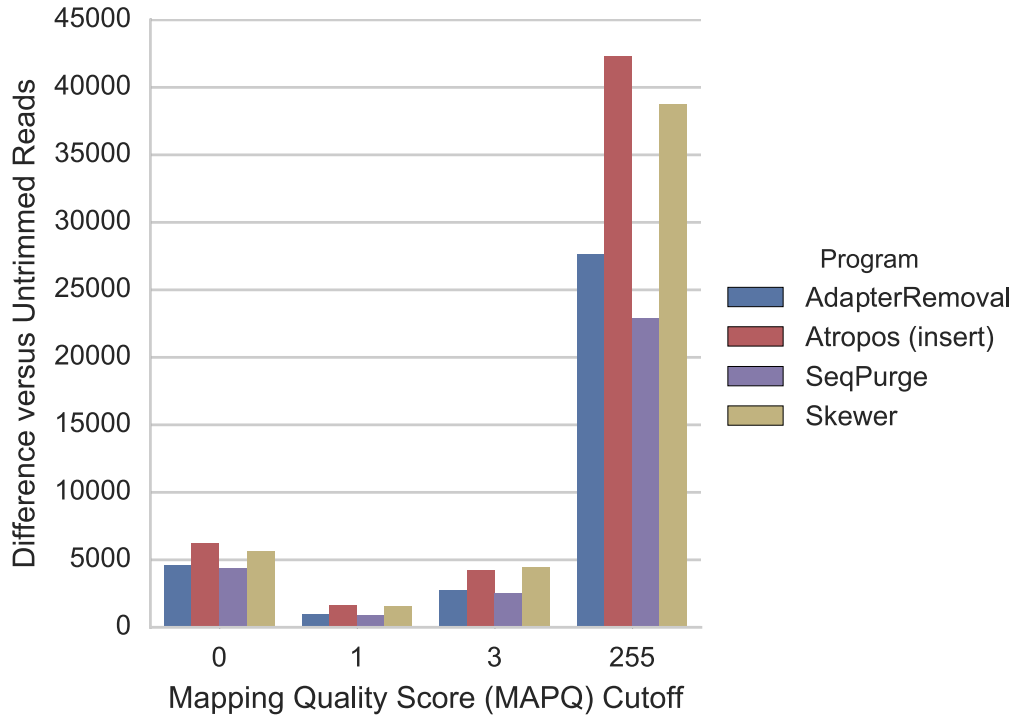


Figure 5. Atropos trimming results in the greatest increase in mRNA-seq reads mapped to GENCODE regions. Reads were adapter-trimmed with all four programs without additional quality trimming. We mapped both untrimmed and trimmed reads to the genome using STAR. When parameter `outSAMmultNmax = 2`, STAR produces only four MAPQ values: 255=unique alignment, 3=two alignments with similar but unequal score; 1=two alignments with equal score; and 0=unmapped. For each MAPQ cutoff $M \in \{0, 1, 3, 255\}$ on the x-axis, the number of trimmed reads that align to GENCODE regions with $\text{MAPQ} \geq M$ less the number of untrimmed reads with $\text{MAPQ} \geq M$ is shown on the y-axis for each program.

398 varying error rates, Atropos (using our new insert-match algorithm) and SeqPurge both demonstrated
 399 overall error rates of 0.01% at the read level, and Atropos has the lowest base-level error rate of 0.0002%.

400 On real WGBS and mRNA-seq data, we found that adapter trimming with Atropos resulted in the
 401 greatest increase in read mapping quality. We also found that stringent quality trimming has a negative
 402 effect on WGBS read mapping quality, at least when using `bwa-meth` as the alignment tool. For reads
 403 trimmed with a quality threshold of 20, all mapping statistics were worse than those for untrimmed reads.

404 In terms of performance, AdapterRemoval and SeqPurge had the best performance of the four tools
 405 tested when only 4 threads were available, while Atropos had superior performance on the simulated
 406 datasets and competitive performance on the real datasets when there were at least 8 threads available. Of
 407 the three write modes, Atropos performed best in parallel-write mode. However, parallel-write mode has
 408 the trade-off of producing a larger number of data files, which may make analyses of large projects more
 409 complicated to manage. Atropos' memory requirements were the highest among the four programs (3-4
 410 GB versus 0.5-1.5 Gb), but well within the capabilities of most modern computer systems.

411 In summary, our results show that Atropos offers the best combination of accuracy and performance
 412 of the tools that we evaluated. Furthermore, Atropos has the richest feature set of the four tools, including
 413 Methyl-Seq-specific trimming options, automated adapter detection, estimation of sequencing error,
 414 computation of quality-control metrics before and after trimming, and support for data generated by many
 415 sequencing methods (ABI SOLiD, Illumina NextSeq, mate-pair libraries, and single-end sequencing).
 416 Although we have not optimized Atropos for long-read data (e.g. PacBio and Nanopore), it should work
 417 on those datasets given appropriate parameter settings, and we plan to soon provide explicit long-read
 418 support.

419 5 DATA AVAILABILITY

- 420 • The Atropos source code, including detailed instructions and all scripts needed to execute the
421 analyses in this paper, are available at <https://github.com/jdidion/atropos>. The
422 portions of Atropos developed by JPD are a work of the US government, and thus all copyright is
423 waived under a CC0 1.0 Universal Public Domain Dedication (<https://creativecommons.org/publicdomain/zero/1.0/>).
424
- 425 • Atropos can be installed using Python 3.3+ and any one of the following methods:
 - 426 – From source, using instructions at the aforementioned GitHub repository website.
 - 427 – From the Python Package Index (pypi), using the pip tool: 'pip install atropos'.
 - 428 – From the Conda package manager: 'conda install atropos'.
 - 429 – From a Docker container, using a Docker or Singularity client: e.g. 'docker run jdidion/atropos'.
430
- 431 • The K562 mRNA-seq data (accession SRR521458) is available from the NCBI Sequence Read
432 Archive: <https://trace.ncbi.nlm.nih.gov/Traces/sra/?run=SRR521458>.
- 433 • The GM12878 WGBS data (accession ENCLB794YYH) is available from the ENCODE project
434 website: <https://www.encodeproject.org/experiments/ENCSR890UQO/>.
- 435 • We used human reference genomes GRCh37 and GRCh38, downloaded from <http://hgdownload.cse.ucsc.edu/downloads.html#human>.
436
- 437 • We used GENCODE v26 annotations, downloaded from ftp://ftp.sanger.ac.uk/pub/genocode/Gencode_human/release_26.
438
- 439 • All datasets, including the simulated DNA-Seq reads, have been packaged into Docker containers,
440 and are available in the Docker Hub (<https://hub.docker.com/r/jdidion/>). Container definitions are
441 available in the aforementioned GitHub repository.

442 6 ACKNOWLEDGEMENTS

443 We thank Jim Mullikin, Stephen Piccolo, and two anonymous reviewers for helpful comments on an
444 earlier version of this manuscript. We also thank the users of Cutadapt and Atropos that have contributed
445 bug reports and improvements. JPD and FSC are funded by the NIH intramural program. Additionally,
446 JPD is funded by the American Diabetes Association (1-17-PDF-100). MM is supported by a grant from
447 the Knut and Alice Wallenberg Foundation to the Wallenberg Advanced Bioinformatics Infrastructure.

448 REFERENCES

- 449 Andrews, S. (2010). FastQC: a quality control tool for high throughput sequence data.
- 450 Bock, C. (2012). Analysing and interpreting DNA methylation data. *Nature Reviews Genetics*, 13(10):705–
451 719.
- 452 Boettiger, C. (2015). An introduction to docker for reproducible research, with examples from the r
453 environment. *ACM SIGOPS Operating Systems Review*, 49(1).
- 454 Del Fabbro, C., Scalabrin, S., Morgante, M., and Giorgi, F. M. (2013). An extensive evaluation of read
455 trimming effects on Illumina NGS data analysis. *PLoS One*, 8(12):e85024–None.
- 456 DePristo, M. A., Banks, E., Poplin, R., Garimella, K. V., Maguire, J. R., Hartl, C., Philippakis, A. A., del
457 Angel, G., Rivas, M. A., Hanna, M., McKenna, A., Fennell, T. J., Kernytsky, A. M., Sivachenko, A. Y.,
458 Cibulskis, K., Gabriel, S. B., Altshuler, D., and Daly, M. J. (2011). A framework for variation discovery
459 and genotyping using next-generation DNA sequencing data. *Nature Genetics*, 43(5):491–498.
- 460 Di Tommaso, P., Chatzou, M., Floden, E. W., Barja, P. P., Palumbo, E., and Notredame, C. (2017).
461 Nextflow enables reproducible computational workflows. *Nat Biotech*, 35(4):316–319.
- 462 Dobin, A., Davis, C. A., Schlesinger, F., Drenkow, J., Zaleski, C., Jha, S., Batut, P., Chaisson, M., and
463 Gingeras, T. R. (2013). STAR: ultrafast universal RNA-seq aligner. *Bioinformatics*, 29(1):15–21.

- 464 Dohm, J. C., Lottaz, C., Borodina, T., and Himmelbauer, H. (2008). Substantial biases in ultra-short read
465 data sets from high-throughput DNA sequencing. *Nucleic Acids Research*, 36(16):e105–e105.
- 466 ENCODE Project Consortium (2012). An integrated encyclopedia of DNA elements in the human genome.
467 *Nature*, 489(7414):57–74.
- 468 Ewels, P., Magnusson, M., Lundin, S., and Käller, M. (2016). MultiQC: Summarize analysis results for
469 multiple tools and samples in a single report. *Bioinformatics*, 32(19):3047–3048.
- 470 Gusfield, D. (1997). *Algorithms on Strings, Trees and Sequences*. Cambridge University Press.
- 471 Harrow, J., Frankish, A., Gonzalez, J. M., Tapanari, E., Diekhans, M., Kokocinski, F., Aken, B. L., Barrell,
472 D., Zadissa, A., Searle, S., Barnes, I., Bignell, A., Boychenko, V., Hunt, T., Kay, M., Mukherjee, G.,
473 Rajan, J., Despacio-Reyes, G., Saunders, G., Steward, C., Harte, R., Lin, M., Howald, C., Tanzer, A.,
474 Derrien, T., Chrast, J., Walters, N., Balasubramanian, S., Pei, B., Tress, M., Rodriguez, J. M., Ezkurdia,
475 I., van Baren, J., Brent, M., Haussler, D., Kellis, M., Valencia, A., Reymond, A., Gerstein, M., Guigó,
476 R., and Hubbard, T. J. (2012). GENCODE: the reference human genome annotation for The ENCODE
477 Project. *Genome research*, 22(9):1760–1774.
- 478 Huang, W., Li, L., Myers, J. R., and Marth, G. T. (2012). ART: a next-generation sequencing read
479 simulator. *Bioinformatics*, 28(4):593–594.
- 480 Jiang, H., Lei, R., Ding, S.-W., and Zhu, S. (2014). Skewer: a fast and accurate adapter trimmer for
481 next-generation sequencing paired-end reads. *BMC Bioinformatics*, 15:182–None.
- 482 Kurtzer, G. M. (2016). Singularity linux application and environment containers for science.
- 483 Martin, M. (2011). Cutadapt removes adapter sequences from high-throughput sequencing reads. *EMB-
484 net.journal*, 17(1):pp. 10–12.
- 485 Martin, M. (2013). *Algorithms and Tools for the Analysis of High-Throughput DNA Sequencing Data*.
486 PhD thesis, TU Dortmund.
- 487 Pedersen, B. S., Eyring, K., De, S., Yang, I. V., and Schwartz, D. A. (2014). Fast and accurate alignment
488 of long bisulfite-seq reads. *arXiv:1401.1129 [q-bio]*. arXiv: 1401.1129.
- 489 Schubert, M., Lindgreen, S., and Orlando, L. (2016). AdapterRemoval v2: rapid adapter trimming,
490 identification, and read merging. *BMC research notes*, 9:88.
- 491 Sturm, M., Schroeder, C., and Bauer, P. (2016). SeqPurge: highly-sensitive adapter trimming for
492 paired-end NGS data. *BMC Bioinformatics*, 17:208.
- 493 Ukkonen, E. (1985). Finding approximate patterns in strings. *Journal of Algorithms*, 6(1):132–137.
- 494 Wang, X. V., Blades, N., Ding, J., Sultana, R., and Parmigiani, G. (2012). Estimation of sequencing error
495 rates in short reads. *BMC Bioinformatics*, 13:185.